



**HAL**  
open science

# Isolated and Bidirectional Three-phase Single-Stage Quad-Active-Bridge Series-Resonant AC-DC converter

Damian Sal y Rosas, Daniel Chavez, Gustavo Navarro, Marcos Lafoz

► **To cite this version:**

Damian Sal y Rosas, Daniel Chavez, Gustavo Navarro, Marcos Lafoz. Isolated and Bidirectional Three-phase Single-Stage Quad-Active-Bridge Series-Resonant AC-DC converter. 2023 25th European Conference on Power Electronics and Applications (EPE'23 ECCE Europe), Sep 2023, Aalborg, Denmark. pp.1-7, 10.23919/EPE23ECCEurope58414.2023.10264528 . hal-04765719

**HAL Id: hal-04765719**

**<https://laas.hal.science/hal-04765719v1>**

Submitted on 4 Nov 2024

**HAL** is a multi-disciplinary open access archive for the deposit and dissemination of scientific research documents, whether they are published or not. The documents may come from teaching and research institutions in France or abroad, or from public or private research centers.

L'archive ouverte pluridisciplinaire **HAL**, est destinée au dépôt et à la diffusion de documents scientifiques de niveau recherche, publiés ou non, émanant des établissements d'enseignement et de recherche français ou étrangers, des laboratoires publics ou privés.

# Isolated and Bidirectional Three-phase Single-Stage Quad-Active-Bridge Series-Resonant AC-DC converter

Damián Sal y Rosas<sup>1,2</sup>; Daniel Chavez<sup>1</sup>; Gustavo Navarro<sup>3</sup>; Marcos Lafoz<sup>3</sup>

<sup>1</sup>UNIVERSIDAD NACIONAL DE INGENIERIA, 210 Tupac Amaru Av. Rimac. Lima, Peru

<sup>2</sup>LAAS-CNRS, University of Toulouse, 31031 Toulouse, France

<sup>3</sup>CIEMAT, Av. Complutense, 40. 28040 Madrid, Spain

dsalyrosas@uni.edu.pe; dachavezo@uni.pe;

## Acknowledgements

This work was financed by CONCYTEC-PROCIENCIA by the project “Manufactura Avanzada de Estaciones de recarga rápida de vehículos eléctricos basada en Sistemas Fotovoltaicos Inteligentes” [Contract N° 007-2021].

## Keywords

«Three-phase», «AC-DC converter», «Bidirectional converters», «Quad-Active-Bridge», «Series-Resonant converter»,

## Abstract

A novel isolated and bidirectional single-stage three-phase AC-DC converter called Quad-Active-Bridge Series-Resonant (QABSR) AC-DC converter is proposed. Unipolar voltage switches are used to modulate the grid voltages. The proposed modulation allows to obtain minimum HF current and a decoupled grid current control. Converter design, simulation and experimental results are presented.

## Introduction

Single-stage (SS) three-phase (3P) AC-DC converters allow bidirectional power flow and galvanic isolation but also have better performances compared to typical two-stage AC-DC converters such as smaller volume, easier control, higher efficiency and longer lifetime [1]. The most popular SS 3P AC-DC converters are based on the Dual Active Bridge (DAB) converter [2] – [4] of which, two of the most representative are shown in Fig. 1

The converter shown in Fig. 1a is composed of three independent single-phase (1P) SS AC-DC converters. Each 1P SS AC-DC converter has a low frequency (LF) synchronous rectifier (SR) cascaded with a DAB DC-DC converter [2].

Therefore, a high number of switches are required which have a high impact in converter efficiency and price. Besides, a time-variant switching frequency and phase-shift (PS) modulation are used to control the grid current. Hence, the modulation and control strategy are very difficult to implement.

The 3P DAB AC-DC converter is shown in Fig. 1b [3]. This converter has fewer switches and uses only one high frequency (HF) transformer, increasing the converter efficiency. However due to usage of bipolar voltage switches (in the matrix converter) to grid modulation, a complex modulation and switches protection have to be considered, which has limited its applicability.

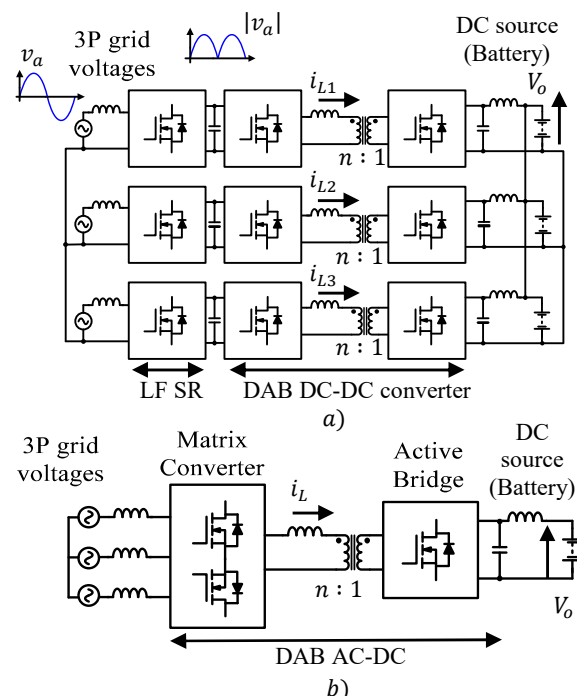


Fig. 1. SS 3P AC-DC converters based on the DAB converter a) Three independent 1P DAB AC-DC converters b) 3P AC-DC DAB converter

To avoid the usage of bipolar voltage switches, the Quad-Active-Bridge (QAB) 3P AC-DC

converter shown in Fig. 2 was introduced in [4], which uses unipolar voltage switches to grid modulation because an offset is added to grid voltages by means of controlling the DC voltage  $V_{OFF}$  in a series-connected capacitor to the grid neutral point (see Fig. 2). Moreover, four PS angles are used to control the power flow ( $\varphi_1, \varphi_2, \varphi_3$  and  $\varphi_4$ ). However, the PS angles calculation and control strategy are very difficult to implement, limiting its applicability.

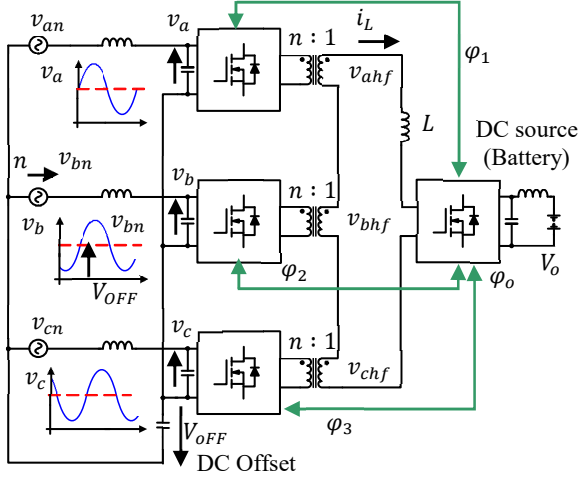


Fig. 2. The QAB 3P AC-DC converter

To overcome the drawbacks above mentioned, a novel SS QAB series-resonant (QABSR) 3P AC-DC converter is introduced in this article. Two main changes in the QAB are proposed. First, a series-resonant circuit is used as a temporary storage element. Hence, a lower HF current is obtained compared to DAB or QAB 3P AC-DC converters where a HF inductor is used [1], [5]. Second, the proposed converter implements duty ratio (DR) and PS modulations with an easier calculation allowing to obtain a HF current with a constant amplitude throughout the grid period. The proposed converter is explained below.

## The proposed QABSR 3P AC-DC converter

The proposed converter is shown in Fig. 3. Three low-pass LC filters with a damping resistor  $r_d$  are used on the AC side. As in the QAB converter, an OFFSET is added in grid voltages by means of controlling the DC voltage  $V_{OFF}$  in capacitor  $C_f$ . Hence, all QAB inputs are DC voltages allowing the usage of unipolar voltage switches to grid voltages modulation. Moreover, three HF transformers are used which are series-connected

on secondary side where a series-resonant circuit (SRC) is placed.

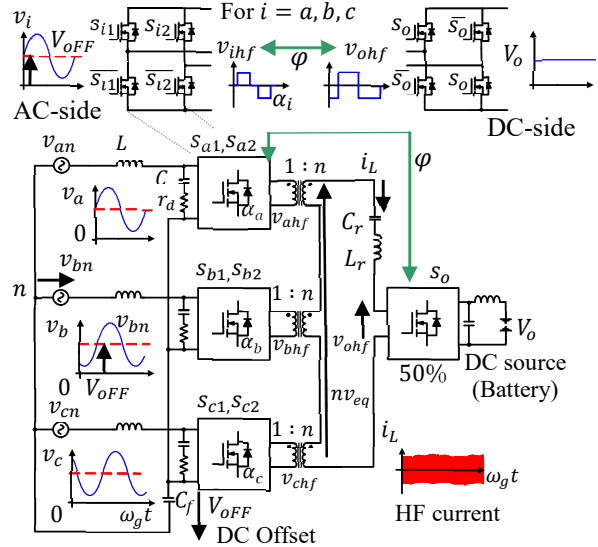


Fig. 3. Proposed QABSR 3P AC-DC converter.

Then, considering a balanced 3P system, the QAB inputs on AC side are given by:

$$v_i = V_{OFF} + v_{in} ; \text{ for } i = a, b, c$$

Where:

$$\begin{cases} v_{an} = V_m \sin(\omega_g t) \\ v_{bn} = V_m \sin(\omega_g t - \frac{2\pi}{3}) \\ v_{cn} = V_m \sin(\omega_g t + \frac{2\pi}{3}) \end{cases} \quad (1)$$

Being  $V_m$  and  $\omega_g$  the grid voltage amplitude and frequency respectively whereas  $V_{OFF}$  is the DC voltage controlled in the capacitor  $C_f$  such that  $V_{OFF} > V_m$  (see Fig. 3).

In proposed modulation three DR angles  $\alpha_a, \alpha_b$  and  $\alpha_c$  and only one phase-shift (PS) angle  $\varphi$  are used as command signals. The modulated voltages at  $\omega_g t = \frac{3\pi}{10}$  are shown in Fig. 4 where the modulation functions are given by:

AC side:

$$\begin{cases} s_{i1} = \text{sgn}\left(\cos\left(\omega_s t - \frac{\alpha_i}{2}\right)\right) \\ s_{i2} = \text{sgn}\left(\cos\left(\omega_s t + \frac{\alpha_i}{2}\right)\right) \end{cases} \text{ for } i = a, b, c \quad (2)$$

DC side:

$$s_o = \text{sgn}(\sin(\omega_s t - \varphi)) \quad (3)$$

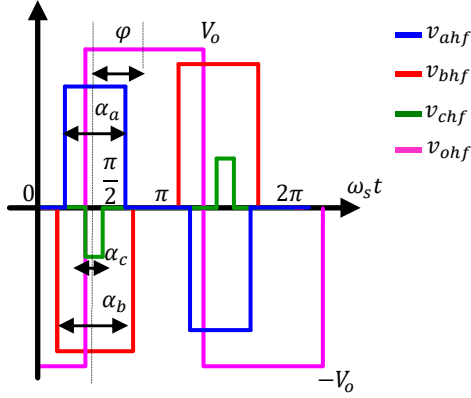


Fig. 4: Proposed modulation

Where  $\omega_s$  is the switching frequency and the function  $sgn(x)$  is defined as [6]:

$$sgn(x) = \begin{cases} 1, & \text{when } x \geq 0 \\ 0, & \text{when } x < 0 \end{cases} \quad (4)$$

Note that, the DR angles  $\alpha_a$ ,  $\alpha_b$  and  $\alpha_c$  are used to modulate the input voltages  $v_a$ ,  $v_b$  and  $v_c$  respectively, generating the HF voltages  $v_{ahf}$ ,  $v_{bhf}$  and  $v_{chf}$ . Whereas, the DC source  $V_o$  is modulated by a 50% symmetrical function generating the HF voltage  $v_{ohf}$  which is phase-shifted  $\varphi$  with respect to  $v_{ahf}$ ,  $v_{bhf}$  and  $v_{chf}$ , as shown in Fig. 4 and Fig. 3.

On the other hand, the SRC is designed as a band-pass filter at switching frequency  $\omega_s$  [5]. Hence, only the components at  $\omega_s$  are considered for power transfer, it means:

For the DC Source:

$$v_{ohf1} = \frac{4}{\pi} V_o \sin(\omega_s t - \varphi); \quad (5)$$

For the grid voltages with OFFSET:

$$v_{ihf1} = \frac{4}{\pi} V_{ihf1} \sin(\omega_s t);$$

Where:

$$V_{ihf1} = v_i \times \sin\left(\frac{\alpha_i}{2}\right); \text{ For } i = a, b, c \quad (6)$$

Being  $v_i = V_{OFF} + v_{in}$  defined in (1) whereas  $\frac{\alpha_i}{2}$  is the correspondent DR angle  $\frac{\alpha_a}{2}$ ,  $\frac{\alpha_b}{2}$  and  $\frac{\alpha_c}{2}$  respectively. In proposed modulation  $\frac{\alpha_i}{2}$  changes linearly with the grid frequency  $\omega_g$  as proposed in [7] it means:

$$\begin{cases} \frac{\alpha_a}{2} = \omega_g t; \\ \frac{\alpha_b}{2} = \omega_g t - \frac{2\pi}{3}; \\ \frac{\alpha_c}{2} = \omega_g t + \frac{2\pi}{3}; \end{cases} \text{ Where } \omega_g t \in [0; 2\pi] \quad (7)$$

Hence,  $V_{ihf1}$  given by (6) can be considered constant during one switching period because  $\omega_s \gg 2\omega_g$ . The series-connection of the HF transformers on the secondary side allows to add the modulated voltages  $v_{ahf}$ ,  $v_{bhf}$  and  $v_{chf}$  given by (6), resulting:

$$nv_{eq1} = \frac{4}{\pi} n \left[ v_a \sin\left(\frac{\alpha_a}{2}\right) + v_b \sin\left(\frac{\alpha_b}{2}\right) + v_c \sin\left(\frac{\alpha_c}{2}\right) \right] \sin(\omega_s t) \quad (8)$$

Hence, replacing (1) and (7) in (8):

$$nv_{eq1} = \frac{4}{\pi} n \left[ \frac{3}{2} V_m \right] \sin(\omega_s t) \quad (9)$$

Where  $V_m$  is the grid voltages amplitude whereas  $n$  is the turns-ratio relationship of HF transformers. Note in (9) that, the voltage  $nv_{eq1}$ , on the secondary side (see Fig.3), has a constant amplitude  $\frac{4}{\pi} n \left[ \frac{3}{2} V_m \right]$ . Therefore, the SRC along with  $n$ , can be sized as an equivalent DABSR DC-DC converter to control the power flow between two DC sources:  $\frac{3}{2} V_m$  and  $V_o$  [7]. Hence,  $n$  and the SRC can be sized as follows:

$$\begin{cases} n = \frac{V_o}{\frac{3}{2} V_m}; & Q = \frac{Z}{\frac{8}{\pi^2} R_o}; & \omega_r = \frac{1}{\sqrt{L_r C_r}}; \\ Z = \sqrt{\frac{L_r}{C_r}}; & F = \frac{\omega_s}{\omega_r}; & R_o = \frac{V_o^2}{P_o} \end{cases} \quad (10)$$

Being  $L_r$  and  $C_r$  the inductance and capacitance of the SRC,  $Q$  and  $\omega_r$  the quality factor and resonance frequency of the SRC,  $P_o$  the nominal power and  $R_o$  the nominal output load.

Then, the average input currents  $\langle i_a \rangle$ ,  $\langle i_b \rangle$  and  $\langle i_c \rangle$ , for one switching period, can be calculated as:

$$\begin{cases} \langle i_a \rangle = [K \sin(\varphi)] \sin\left(\frac{\alpha_a}{2}\right); \\ \langle i_b \rangle = [K \sin(\varphi)] \sin\left(\frac{\alpha_b}{2}\right); \\ \langle i_c \rangle = [K \sin(\varphi)] \sin\left(\frac{\alpha_c}{2}\right); \end{cases} \quad (11)$$

Where:

$$K = \frac{8nV_o}{\pi^2 Z \left(F - \frac{1}{F}\right)} \quad (12)$$

Being the DR angles  $\frac{\alpha_a}{2}, \frac{\alpha_b}{2}, \frac{\alpha_c}{2}$  given by (7). Note in (11) that, the factor  $K \sin(\varphi)$  is repeated in the three average currents whereas, each average current depends on its respectively DR angle given by (7) which controls the angle of the grid current. Hence,  $\varphi$  can be used to control the grid current amplitude. Then, considering a balanced 3P currents given by:

$$\begin{cases} i_{bn} = I_m \sin(\omega_g t); \\ i_{bn} = I_m \sin\left(\omega_g t - \frac{2\pi}{3}\right); \\ i_{cn} = I_m \sin\left(\omega_g t + \frac{2\pi}{3}\right); \end{cases} \quad (13)$$

The PS angle  $\varphi$  can be calculated as:

$$\varphi = \text{asin}\left(\frac{I_m}{K}\right) \quad (14)$$

Where  $I_m$  is the grid current amplitude and  $K$  is defined in (12). Note that, with the proposed modulation, a decoupled grid current control can be implemented for each grid current, using the DR angles  $\frac{\alpha_a}{2}, \frac{\alpha_b}{2}, \frac{\alpha_c}{2}$  and  $\varphi$ .

## Simulation results

The proposed converter was validated by simulation using the parameters of Table I.

**Table I: Converter parameters**

Item	Value	Item	Value
Output Voltage and Power ( $V_o, P_o$ )	400V, 2 kW	Tank circuit ( $L_r, C_r$ )	380 $\mu$ H, 5.5 $\eta$ F
Grid Voltage	220V RMS, 60 Hz	Turns-ratio relationship (1: n)	1: 0.86
Switching frequency ( $f_s$ )	120 kHz	Tank circuit parameters ( $F, Q$ )	$F = 1.1$ , $Q = 4$
OFFSET $V_{OFF}$ and $C_f$	350V, 4.7 $\mu$ F	LC Input Filter ( $L_i, C_i, r_d$ )	200 $\mu$ H, 1 $\mu$ F, 1.1 $\Omega$

Note in table I that the series-connected capacitor  $C_f$  in grid neutral point takes a small capacitance value ( $C_f = 4.7\mu\text{F}$ ) unlike a DC-link capacitor used in two-stage AC-DC converters. Moreover,  $V_{OFF} (350\text{V}) > V_m (220\sqrt{2})$ .

In Fig. 5 are shown the 3P grid currents, the DC output current  $i_o$ , the scaled grid voltage  $v_{an}/20$  and the grid voltage with OFFSET  $v_a/20$  (where  $v_a = v_{an} + V_{OFF}$ ) considering the nominal power and bidirectional power flow: grid-to-battery (G2B) and battery-to-grid (B2G). Very low THD is obtained in the grid currents which are controlled by PI controllers as well as the DC voltage  $V_{OFF}$  in capacitor  $C_f$ .

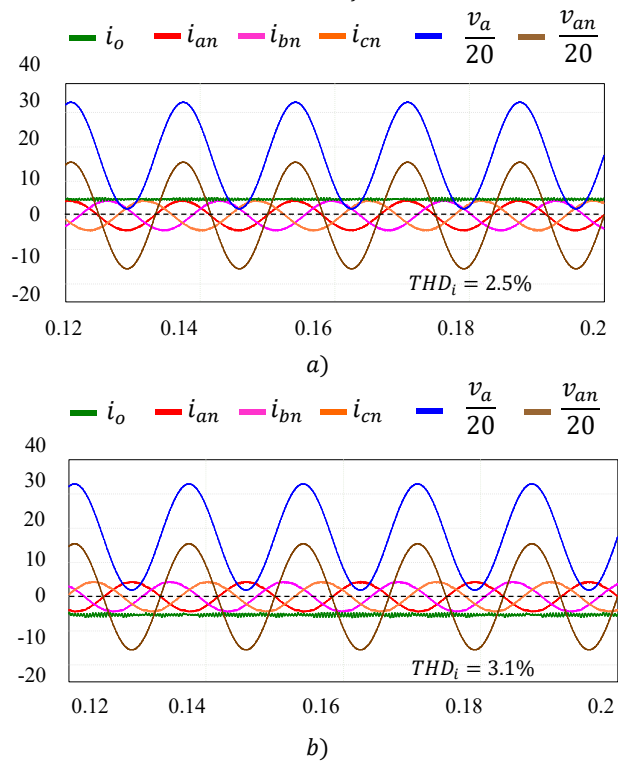


Fig. 5: Grid currents and DC output current for bidirectional power flow. a) G2B. b) B2G.

On the other hand, note in Fig. 6(a) that even if the QABSR inputs on the AC side have high ripple (almost 100%), the HF current  $i_L$  has a constant amplitude throughout the grid period, obtaining a 3P HF power decoupling in the SRC [7].

Finally, in Fig. 6(b) all active bridges in the QABSR converter can achieve ZVS mode. Therefore, high efficiency is obtained. However, for G2B power flow, the ZVS mode is lost on AC-side when  $\alpha_a, \alpha_b$  and  $\alpha_c$  take small angle values.

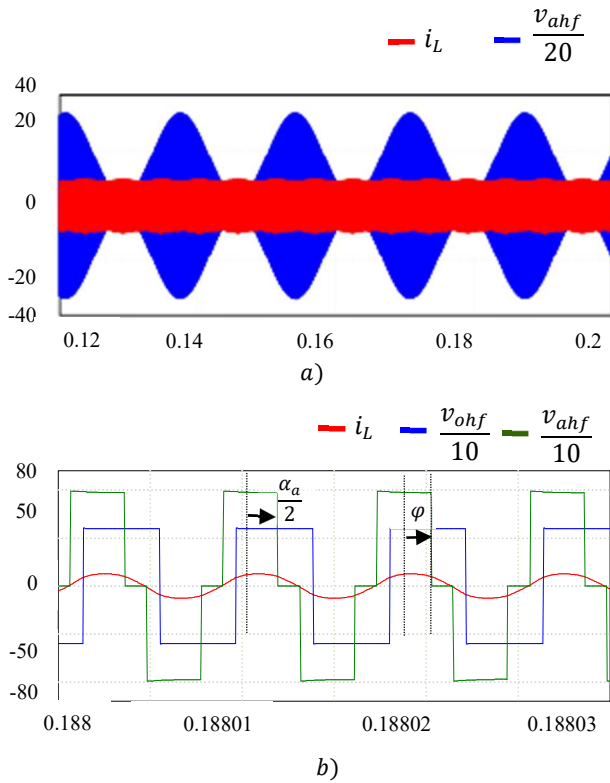


Fig. 6: Modulated grid voltages and HF current a) For five grid periods. b) For three switching periods and evaluated at  $\omega_g t = \frac{\pi}{3}$ .

### Experimental results

The proposed converter was validated using the components of Table I.

The experimental setup is shown in Fig. 7. To validate the bidirectional power flow in the grid, a 3Ø AC source and a 3Ø resistive load in parallel were used. Similarly, a bidirectional source was used on the DC side.

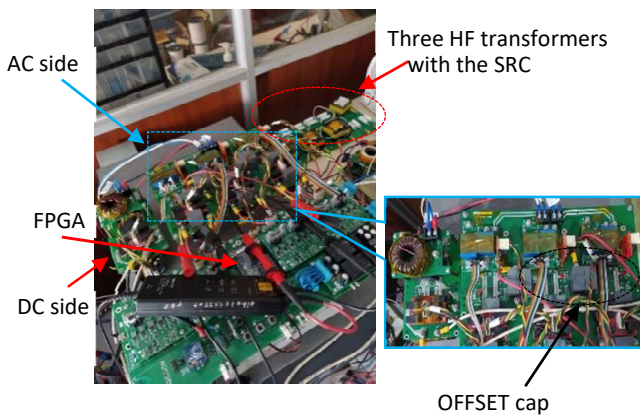


Fig. 7: The experimental setup for 2kW.

In Fig. 8 and 9 are shown the 3P grid currents, the DC output current  $i_o$ , for G2B and B2G respectively. A very low THD was obtained along with high efficiency. Note that, for B2G the THD is lower than G2B mode. Moreover, the efficiency in G2B is lower than B2G mode (95.4% vs 96.2%). This decrease in the efficiency is because ZVS mode is lost in one leg of the ABs on the AC side for G2B when the DR angles  $\alpha_a, \alpha_b, \alpha_c$  take small angle values. The resulting HF current along with the modulated voltages for the grid voltage  $v_a$  are shown in Fig. 10 and Fig. 11 for G2B and B2G.

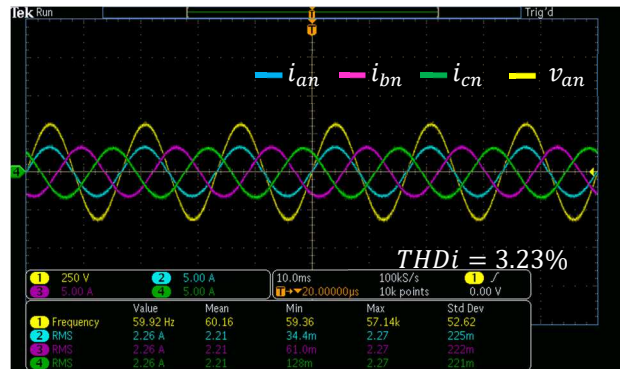


Fig. 8: Grid currents for G2B.

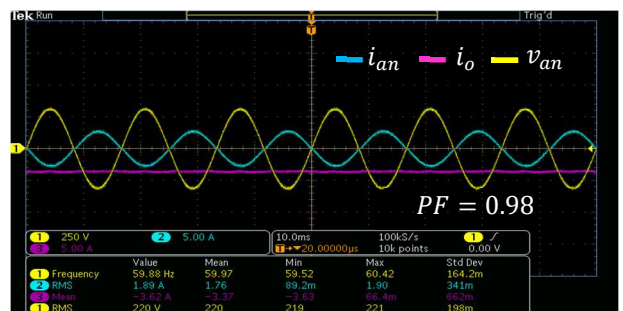
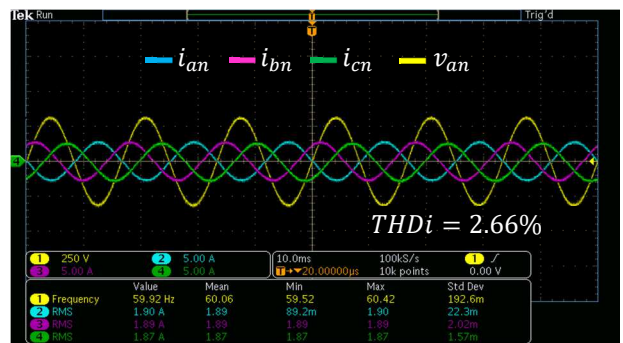


Fig. 9: Grid and DC output currents for B2G.

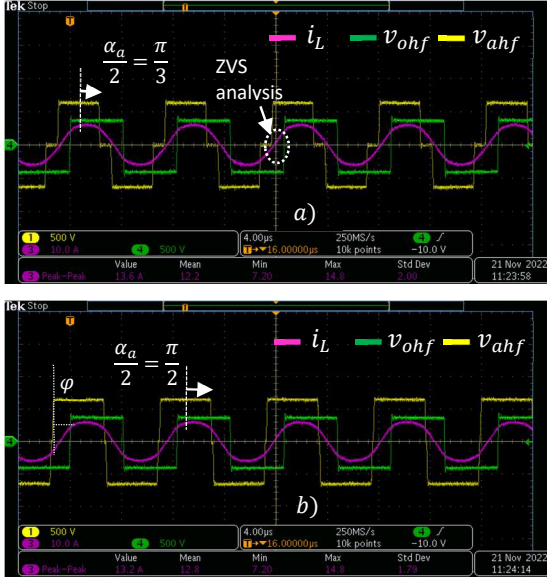


Fig. 10: Modulated grid voltages and HF current for G2B: a)  $\omega_g t = \frac{\pi}{3}$  b)  $\omega_g t = \frac{\pi}{2}$

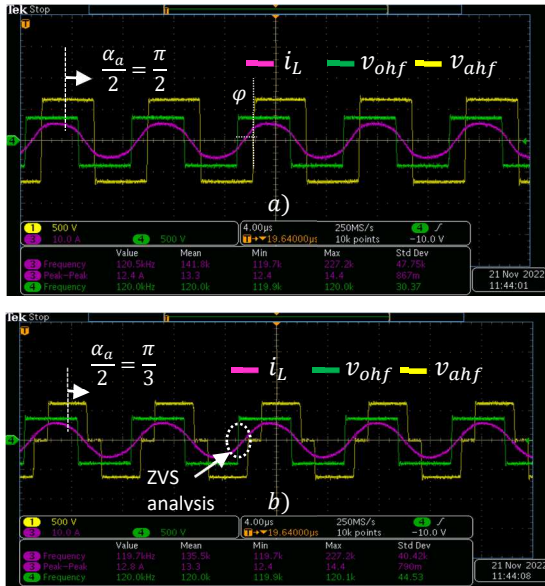


Fig. 11: Modulated grid voltages and HF current for B2G: a)  $\omega_g t = \frac{\pi}{2}$  b)  $\omega_g t = \frac{\pi}{3}$ .

Note in Fig. 10 and Fig. 11 that ZVS mode is obtained for G2B and B2G when the DR  $\frac{\alpha_a}{2}$  is close to  $\frac{\pi}{2}$ . Nevertheless, as shown in Fig.10a, ZVS mode will be lost in one leg of the Active bridge when  $\frac{\alpha_a}{2}$  takes small angles values.

Finally, the HF 3P power decoupling is validated in Fig. 12 where the modulated voltages  $v_{ahf}$ ,  $v_{bhf}$ ,  $v_{chf}$  and the HF current  $i_L$  are shown for three grid periods. Note in Fig. 12 that, the HF current has a constant amplitude throughout the grid period.

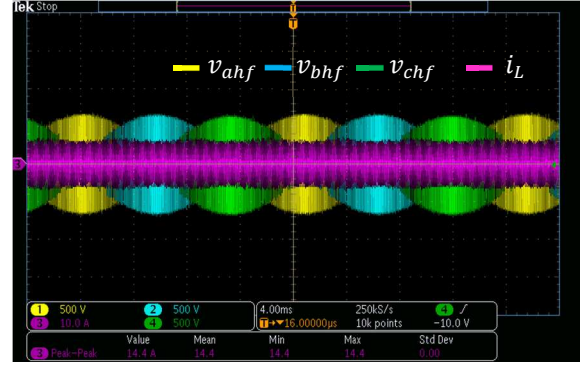


Fig. 12: Modulated grid voltages and HF current in the tank circuit for three grid periods.

## Comparison with QAB structure

A brief comparison with a similar single-stage AC-DC structure [4] is shown in Table 2.

Table II: Comparison with QAB converter

Parameters	Proposed QABSR	QAB structure [4]
Storage Element	1 SRC	1 HF inductor
Modulation	3 DR angles with 1 PS angle	4 PS angles
Switching Frequency	High	Medium
LC AC filter	Smaller	Medium
Control complexity	Low	High
Power Density	High	High
$THD_i$	2.66%	6%
Efficiency	96%	Not reported

The proposed converter has smaller  $THD_i$  and AC filters compared with QAB converter. Smaller AC filters can be used because a higher switching frequency can be used. Moreover, the control strategy and modulation are easier to implement. However, the drawback of the proposed converter is the usage of resonant capacitors (in the tank

circuit) which increase the converter volume compared to a DAB structure [1].

## Conclusion and Future works

A novel single-stage 3P AC-DC converter is proposed in this article called QABSR 3P AC-DC converter. A novel QAB AC-DC modulation is introduced where the grid voltages with the DC offset are modulated by duty ratio modulation. Whereas, the DC source is modulated by a 50% symmetrical function, which is phase-shifted with respect to modulated grid voltages with OFFSET. Bidirectional power flow, a decoupled grid currents control and a three-phase power decoupling in the HF current have been validated. The proposed modulation allows to obtain a HF current with a constant amplitude and smaller value throughout the grid period compared with other single-stage AC-DC structures. Besides, ZVS mode is achieved in all active bridges achieving high efficiency. Hence, the proposed converter is a good candidate for single-stage AC-DC converter particularly when bipolar voltage switches have to be avoided.

## References

- [1]. Fengjiang Wu, Kaixuan Wang, Guangfu Hu, Yang Shen and Suhua Luo, "Overview of Single-Stage High-Frequency Isolated AC-DC Converters and Modulation Strategies", IEEE TRANS. ON POWER ELECTRONICS, VOL. 38, NO. 2, pp. 1583-1598, FEB. 2023
- [2]. Juncheng Lu, Kevin Bai, Allan Ray Taylor, Guanliang Liu, Alan Brown, Philip Johnson and Matt McAmmond, "A Modular-Designed Three-Phase High-Efficiency High-Power-Density EV Battery Charger Using Dual/Triple-Phase-Shift Control", IEEE TRANS. ON POWER ELECTRONICS, VOL. 33, NO. 9, pp. 8091 – 8100, SEP. 2018
- [3]. Lukas Schrittwieser, Michael Leibl and Johann W. Kolar. "99% Efficient Isolated Three-Phase Matrix-Type DAB Buck-Boost PFC Rectifier", IEEE TRANS. ON POWER ELECTRONICS, VOL. 35, NO. 1, JAN. 2020
- [4]. Bas Vermulst, Jorge L. Duarte, Cornelis G. E. Wijnands and Elena Lomonova, "Quad-Active-Bridge Single-Stage Bidirectional Three-Phase AC-DC Converter with Isolation: Introduction and Optimized Modulation", IEEE TRANS. ON POWER ELECTRONICS, VOL. 32, NO. 4, pp. 2546-2557, APRIL 2017.
- [5]. Damian Sal y Rosas, Jherson Andrade, David Frey and Jean-Paul Ferrieux "Single Stage Isolated Bidirectional DC/AC Three-phase Converter with a Series-resonant Circuit for V2G", in Proc. of VPPC, Dec. 2017.
- [6]. Hariharan Krishnaswami and Shesh Narayan Vaishnav, "Single-stage Isolated Bidirectional Converter Topology using High Frequency AC link for Charging and V2G Applications of PHEV" in Proc. of VPPC, pp. 1-4, Sep. 2011.
- [7]. Damian Sal y Rosas, Daniel Chavez, D. Frey, JP. Ferrieux, "Single-Stage Isolated and Bidirectional Three-Phase Series-Resonant AC-DC Converter: Modulation for Active and Reactive Power Control", in Energies Journal, 15(21), 8070, <https://doi.org/10.3390/en15218070>, OCT. 2022.